



Structure and electronic properties of the nanopeapods—One dimensional C₆₀O polymer encapsulated in single-walled carbon nanotubes

Weiye Qiao^a, Xinqian Li^b, Hongcun Bai^a, Ying Zhu^a, Yuanhe Huang^{a,*}

^a College of Chemistry, Beijing Normal University, Beijing 100875, China

^b Institute for Materials Chemistry and Engineering and International Research Center for Molecular Systems, Kyushu University, Fukuoka 819-0395, Japan

ARTICLE INFO

Article history:

Received 9 October 2011

Received in revised form

22 November 2011

Accepted 26 November 2011

Available online 4 December 2011

Keywords:

C₆₀O

Stability

Mobility

Peapod

Carbon nanotube

Self-consistent field crystal orbital

ABSTRACT

The structure–property relationship of the nanopeapods—one dimensional (1D) C₆₀O polymer encapsulated in single-walled carbon nanotubes (SWCNTs)—is studied by means of the self-consistent field crystal orbital method. The calculations show that the nearest distance between the two constituents is within Van der Waals interaction scope in the most stable two peapods. The SWCNT sizes affect not only the stability but also the electronic structures of the peapods. The peapods with larger tube diameters keep the semiconductive and metallic properties of the corresponding pristine SWCNTs. These combination systems are stiffer than the corresponding SWCNTs due to larger Young's moduli. The magnitude order of the calculated mobility of charge carriers is in the range of 10²–10⁵ cm² V⁻¹ s⁻¹ for the peapods, indicating that the combined systems may be good high-mobility electronic materials.

© 2011 Elsevier Inc. All rights reserved.

1. Introduction

Since the discovery of carbon nanotubes (CNTs) in 1991 [1], scientists have paid much attention to their unique chemical and physical properties [2–6]. Due to the special surface structure and ideal cylindrical one dimensional (1D) empty cavity, the doping CNTs by adsorbing or encapsulating various materials on the exterior surface or into the interior 1D empty cavity have been an important aspect for the theoretical and experimental studies [7–12]. In the confinement environment of the 1D cavity, the encapsulated guest molecules may form novel structures which are different from their form in the bulk condition [13,14]. For example, the single, double and triple helical structures of iodine can be formed in the single-walled carbon nanotubes (SWCNTs) [15], whereas iodine exists as the orthorhombic crystals in the bulk condition.

Since C₆₀ molecules were first introduced into the SWCNTs by the laser ablation [16], the peapods filled with C₆₀ molecules have been one of the systems, which are studied most-widely both theoretically and experimentally [17–21]. Under electron irradiation or thermal annealing, the C₆₀ molecules in the SWCNTs can coalesce with each other and finally form the stable and corrugated peanut nanotubes [22]. In 2004, one kind of novel unbranched covalent 1D C₆₀O polymer in the SWCNTs was

observed. The C₆₀ cages in the SWCNTs are linked periodically head to tail by the furan-type bridge shown in the High Resolution Transmission Electron Microscopy (HRTEM) micrograph [23]. However, the detailed structure and properties of the novel 1D C₆₀O polymer encapsulated in SWCNT is still not clear so far. A theoretical study would help understand the possible structures and electronic properties of the peapods, which are denoted as (C₆₀O)_{pol}@SWCNT in the following (the lower-case subscript pol is the abbreviation of polymer). In this paper, we construct several possible structures of the combination systems with the 1D C₆₀O polymer encapsulated into the zigzag and armchair SWCNTs with different diameters. We want to know what properties these (C₆₀O)_{pol}@SWCNTs have and whether the encapsulation can improve the structure and electronic properties, compared with the original constituents forming the combined systems. The self-consistent field crystal orbital (SCF-CO) calculations based on density functional theory (DFT) are carried out to probe the structure–property relationship of the (C₆₀O)_{pol}@SWCNTs. The theoretical study on these peapods should also be helpful for the possible practical application of the novel material.

2. Models and computational methods

As is shown in the HRTEM micrograph in the experiment, the individual C₆₀ cages in the SWCNTs are linked head to tail by the furan-type bridge periodically. We have ever constructed several 1D C₆₀O polymers through the furan-bridge connection and the

* Corresponding author. Fax: +86 10 58802075.

E-mail address: yuanhe@bnu.edu.cn (Y. Huang).

most stable one ($P1$) with the symmetry of C_{2V} is illustrated in Fig. 1, which is also selected as the inner $C_{60}O$ polymer of the peapods in our studies. The sign 6/6 in Fig. 1 denotes the C–C bond in the C_{60} cages (shared by two hexagons), which construct two edges of the furan ring bridges. It is well known that the environment around those bonds in the C_{60} cages concerned with the formation of intercage bonds would affect strain release and reactive activity of the C–C bonds. More pentagons around these C–C bonds in the C_{60} cage would introduce more strain and higher reactivity [24]. Around the 6/6 bond there are two pentagons and two hexagons, but there are three hexagons and one pentagon around the 5/6 bond. $P1$ is most stable because the sides of the furan rings are all 6/6 bonds. In the other constructed 1D $C_{60}O$ polymers with the head to tail linking structure, at least one of the furan sides is 5/6 bond. The selected zigzag tubes are SWCNTs ($n,0$) $n=14, 16, 18, 20, 22$ and the armchair tubes are SWCNTs (m,m), $m=10, 12$. It would be interesting in how the tube sizes affect the stabilities and electronic properties of the peapods. Here n and m are taken as even number for keeping the symmetry of $(C_{60}O)_{\text{pol}}@SWCNTs$ as C_{2V} the same as that of the 1D $C_{60}O$ polymer and saving computational cost. The tube diameters of the $(C_{60}O)_{\text{pol}}@SWCNTs$ are in the range of 13.6–14.9 Å estimated from the experiment [23], which are close to those of SWCNT(10,10) and SWCNT(18,0) (13.56 Å and 14.10 Å, respectively).

Here a commensurability condition of the 1D periodicity between the SWCNTs and the 1D $C_{60}O$ polymer is imposed, which means that both SWCNTs and the 1D $C_{60}O$ polymer in the peapods have the same lattice constants or the same translational length. One unit cell contains two $C_{60}O$ and four unit cells of the corresponding pristine SWCNT (2 oxygen and $120+16n$ carbon atoms) for the zigzag peapod $(C_{60}O)_{\text{pol}}@(n,0)$, but two $C_{60}O$ units and eight unit cells of the corresponding pristine SWCNT (2 oxygen and $120+32m$ carbon atoms) for the armchair peapod $(C_{60}O)_{\text{pol}}@(m,m)$. Although calculation based on the commensurability condition has some artificial effects, the commensurability condition has been successfully applied to the discussions of many 1D periodic systems, such as nanowires enclosing the carbon atom chain [25,26], peapods encapsulating C_{60} molecules [27–29] and so on.

Computations are performed using the ab initio SCF-CO method based on Perdew–Burke–Ernzerhof (PBE) [30] DFT with CRYSTAL06 program [31]. The geometric structures are fully optimized at 3–21 G* level, while the band structures and density of states of the peapods are calculated with 6–21 G* basis set, which is implemented in the CRYSTAL06 program for the solid state calculations. In the SCF-CO calculations, shrinking factors are set to 40, and default values of convergence criteria in CRYSTAL06 program are

used. The optimized structures of the 1D $C_{60}O$ polymer and three representative peapods are given in Fig. 1.

3. Results and discussions

3.1. Structures and stabilities

The optimized distance between the two neighboring C_{60} cages is about 10 Å for the armchair peapods and the distance is about 8.6 Å for zigzag peapods, therefore in the constructed models, the stack of $C_{60}O$ in the zigzag SWCNTs is tighter than in the armchair SWCNTs. The distance between the two neighboring C_{60} cages in the isolated 1D $C_{60}O$ polymer, 9.3 Å, are longer and shorter than those in the zigzag peapods and armchair peapods, respectively. The bond length changes in the middle part of the C_{60} cages are less than 0.03 Å. These show that the encapsulation has larger influence on the intercage bond lengths between the neighbor C_{60} cages, which should also be partial reflection of the commensurability condition.

The binding energy E_b per unit cell is defined as

$$E_b = E_{\text{peapod}} - E_{1D C_{60}O} - E_T, \quad (1)$$

where E_{peapod} , $E_{1D C_{60}O}$ and E_T are the energies per unit cell for the peapods, the inner 1D $C_{60}O$ polymer and the outer corresponding carbon nanotube, respectively. We would like to mention again that a unit cell of the outer carbon nanotubes in the peapods contains four and eight cells of the pristine zigzag and armchair nanotubes, respectively. From Table 1, it can be seen that the binding energies are -0.689 eV/cell and -0.481 eV/cell for $(C_{60}O)_{\text{pol}}@(18,0)$ and $(C_{60}O)_{\text{pol}}@(10,10)$, respectively. The minus binding energies show that the encapsulation is energetically favorable for the formation of the two peapods. It is found that

Table 1

Calculated deformation and binding energies (eV/cell), Young moduli (TPa) for the peapods $(C_{60}O)_{\text{pol}}@(n,m)$.

Peapods	ΔE_{d1}	ΔE_{d2}	E_b	Y
$(C_{60}O)_{\text{pol}}@(14,0)$	8.791	7.456	20.555	1.566
$(C_{60}O)_{\text{pol}}@(16,0)$	3.364	0.305	2.436	1.391
$(C_{60}O)_{\text{pol}}@(18,0)$	3.252	0.158	-0.689	1.285
$(C_{60}O)_{\text{pol}}@(20,0)$	3.286	0.092	-0.009	1.142
$(C_{60}O)_{\text{pol}}@(22,0)$	3.205	0.294	0.221	0.973
$(C_{60}O)_{\text{pol}}@(10,10)$	1.693	0.091	-0.481	1.220
$(C_{60}O)_{\text{pol}}@(12,12)$	1.746	0.050	0.260	1.212

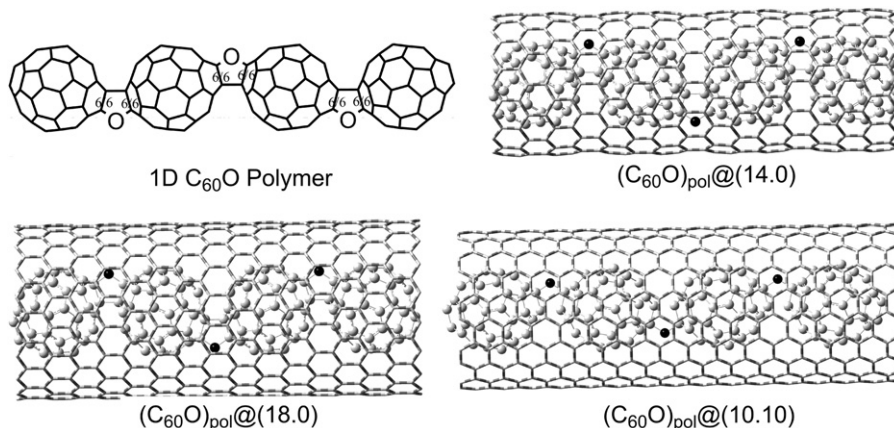


Fig. 1. Optimized structures of the 1D $C_{60}O$ polymer and three representative peapods.

the stability of the peapods is closely related to the distance between the two components. The nearest distance between $C_{60}O$ and tube wall are 3.51 Å and 3.35 Å for $(C_{60}O)_{\text{pol}}@ (18,0)$ and $(C_{60}O)_{\text{pol}}@ (10,10)$, respectively, indicating that the main interaction is Van der Waals interaction between the SWCNTs and 1D $C_{60}O$ polymers. This also indicates that the dispersion interaction has important influence on the stability of the peapods. Moreover, the binding energies become positive for the peapods with smaller tube diameters such as $(C_{60}O)_{\text{pol}}@ (n,0)$ ($n < 18$), as well as the peapods with larger tube diameters, $(C_{60}O)_{\text{pol}}@ (22,0)$ and $(C_{60}O)_{\text{pol}}@ (12,12)$. Hence the most favorable tubes for the encapsulation of the 1D $C_{60}O$ polymer should be those with suitable hollow, which can keep the distance between the two constituents within the Van der Waals scope. Just as reported in the previous researches [32,33], the space in the nanotubes indeed plays a very important role in the thermodynamic stabilities of the combined systems.

As shown in Fig. 1, the tube silhouette becomes obviously undulating for the $(C_{60}O)_{\text{pol}}@ (14,0)$, which is the smallest peapod studied here. The nearest distance between the wall of tube and the atoms of C_{60} cage is about 2.50 Å for $(C_{60}O)_{\text{pol}}@ (14,0)$, which is much smaller than the Van der Waals interaction distance. There exists strong repulsive interaction between the two components, resulting significant deformation of both the C_{60} cages and SWCNT(14,0). The difference of tube diameter between the thinnest and the thickest parts is about 0.5 Å for $(C_{60}O)_{\text{pol}}@ (14,0)$, whereas it is smaller than 0.14 Å for the other peapods. In $(C_{60}O)_{\text{pol}}@ (14,0)$, some bond lengths of the tube are stretched to 1.48 Å and the

difference between the longest C–C bond length and the shortest one on the tube wall is 0.05 Å, while the difference is smaller than 0.007 Å for the other peapods. The degree of structure deformation for the peapods with larger tube diameters is smaller because of weaker interaction between the two constituents.

The deformation energies of the 1D $C_{60}O$ polymer (ΔE_{d1}) and SWCNTs (ΔE_{d2}) are defined as $\Delta E_{d1} = E_{d1} - E_{1D C_{60}O}$ and $\Delta E_{d2} = E_{d2} - E_r$, respectively. E_{d1} , E_{d2} are the energies per unit cell of the deformed 1D $C_{60}O$ polymer and corresponding SWCNTs in the peapods. The calculated results are also shown in Table 1.

We can see that $(C_{60}O)_{\text{pol}}@ (14,0)$ with the smallest tube diameter has the largest deformation energy. As a whole, the deformation energies of the peapods decrease with the increase of the tube diameters. Moreover, the deformation energies of the 1D $C_{60}O$ polymer are larger than those of the SWCNTs for all the peapods. This reflects that the interaction between the two constituents has larger influence on the structure deformation for the 1D $C_{60}O$ polymer than for the corresponding SWCNTs.

3.2. Young's moduli

The calculation of Young's modulus (Y) is based on the elastic stiffness of the 1D system using the second derivative of the strain energy of a unit cell with respect to the axial strain:

$$Y = \frac{1}{V_0} \left. \frac{\partial^2 E}{\partial \varepsilon^2} \right|_{\varepsilon=0} \quad (2)$$

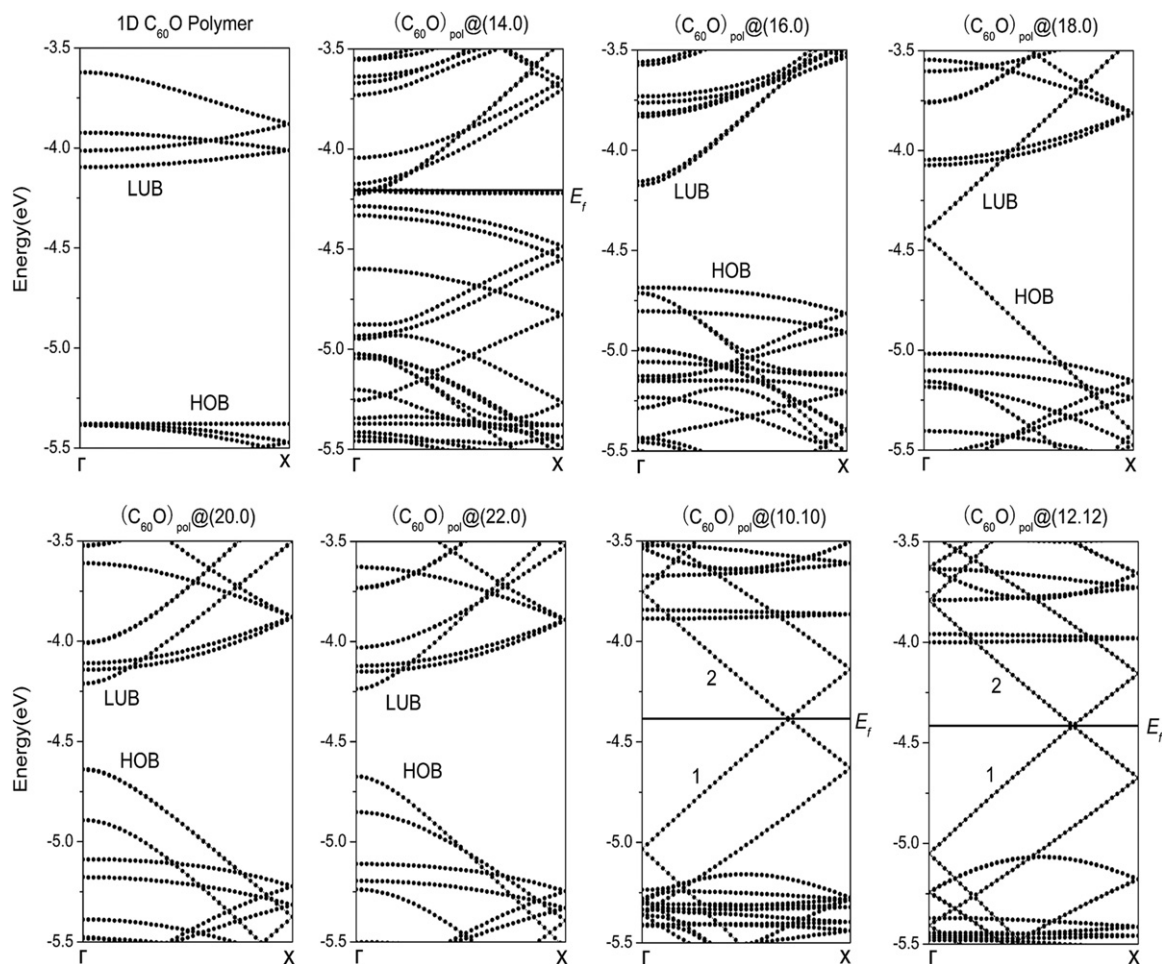


Fig. 2. Band structures of the peapods and the 1D $C_{60}O$ polymer.

where V_0 is the volume of a unit cell, E is the strain energy and ε is a small deformation of the lattice constants defined as $\varepsilon = (L - L_0)/L_0$. L_0 and L are the lengths of the unit cell before and after the strain, respectively. We calculate the energies of the unit cell at $\varepsilon = \pm 0.4\%$, $\pm 0.2\%$ and $\pm 0.1\%$. Then we fit the curve of strain energy with respect to the values of ε with the correlation coefficient > 0.99 and get the second derivative. Thus Y can be obtained according to Eq. (2) and are also listed in Table 1.

The calculated Young's moduli of these peapods are in the range of 0.973–1.566 TPa. It can be seen that the Young moduli decrease monotonically with the increase of the carbon tube diameters, which is different from the variation of the binding and deformation energies. This is due mainly to larger space between the 1D $C_{60}O$ polymer and the corresponding SWCNTs with increase of SWCNT diameters, which results in smaller average atom distribution density and Young moduli. Young's moduli of the pristine SWCNTs are calculated to be about 1 TPa with the same methods, which are in agreement with the values reported in the experimental and theoretical researches [34–36]. Besides, the Young's modulus of the 1D $C_{60}O$ polymer is 0.195 TPa with same calculation method. By comparison, we find that the combined systems have larger Young's moduli than both of the two constituents, indicating that the encapsulation of the 1D $C_{60}O$ polymer can enhance the resistance to the stress along the tube axis for the SWCNTs. However, the filling would not always make the SWCNTs stiffer. For instance, it is reported that the tubes encapsulating separately distributed C_{60} molecules were slightly softer than the undoped ones [37].

3.3. Electronic properties

The calculated band structures of $(C_{60}O)_{\text{pol}}@SWCNTs$ are given in Fig. 2 and the derived electronic properties are listed in Table 2. For the comparison, the band structure of the 1D $C_{60}O$ polymers is also shown in Fig. 2. From Fig. 2, it can be seen that the $(C_{60}O)_{\text{pol}}@(n,0)$ s are semiconductors with the energy gaps occurring in the center of Brillouin zone except for $(C_{60}O)_{\text{pol}}@(14,0)$. Here the energy gap (E_g) is the difference between top of the highest occupied band (HOB) and bottom of the lowest unoccupied band (LUB). It is well known that the zigzag tubes are semiconductors. Here SWCNT(18,0) has near zero E_g of 0.014 eV due to satisfying $2n+m=3l$ rule (l is a interger). The 1D $C_{60}O$ polymer has also an energy gap as shown in Fig. 2. Hence, the semiconductive properties of the two constituents are kept for the encapsulation of the 1D $C_{60}O$ polymer into zigzag SWCNTs ($n,0$) for those peapods with larger tube diameters. Moreover, compared with the band structure of the isolated 1D $C_{60}O$ polymer, those flatter bands, which mainly derive from the 1D $C_{60}O$ polymer are lift in the peapods. This is an important factor resulting in metallic $(C_{60}O)_{\text{pol}}@(14,0)$, in which two of partially filled bands are the 1D $C_{60}O$ polymer-derived bands. The HOB of $(C_{60}O)_{\text{pol}}@(16,0)$ is also the 1D $C_{60}O$ polymer-derived band. But

the HOBs are all the SWCNT-derived and the lowest 1D $C_{60}O$ polymer-derived empty bands become close to the LUBs derived from the SWCNTs for $(C_{60}O)_{\text{pol}}@(n,0)$ ($n > 16$). With the increase of the tube diameters, the 1D $C_{60}O$ polymer-derived bands fall and shift toward to original position in the 1D $C_{60}O$ polymer, indicating weakened interaction between the two constituents. As to the armchair peapods, both $(C_{60}O)_{\text{pol}}@(12,12)$ and $(C_{60}O)_{\text{pol}}@(10,10)$ have metallic property with zero energy gaps. The two frontier bands overlap and become partially filled, similar to the case in the pristine armchair SWCNTs. These results manifest that the encapsulation cannot change the semiconductive or metallic properties for the corresponding SWCNTs with larger diameters. However, when the C_{60} cages are encapsulated into SWCNT(18,0), the combined peapod becomes a metallic system [38]. Therefore, different filling may lead to different modulation of the electronic properties for the same SWCNT.

As a matter of fact, the band structures of the peapods with larger tube diameters ($(C_{60}O)_{\text{pol}}@(n,0)$, $n=18, 20, 22$), $(C_{60}O)_{\text{pol}}@(10,10)$ and $(C_{60}O)_{\text{pol}}@(12,12)$ can almost be considered as the simple overlap of the two constituent bands. In these five peapods, the nearest distance between the two constituents is larger than 3.3 Å, resulting in weaker interaction between the two constituents. Because of the weaker interaction the shapes and character of energy bands are kept in the combined systems for the two constituents. The frontier bands all derive from the corresponding SWCNTs. In fact, the values of energy gaps are almost the same as those of the corresponding SWCNTs.

For $(C_{60}O)_{\text{pol}}@(14,0)$, the shape of bands originating from both components changes remarkably due to stronger interaction between the two components. The stronger interaction even leads to the overlap of the frontier bands, altering the semiconductive properties of the two components. However, the encapsulation of the 1D $C_{60}O$ polymer into the SWCNT (14,0) is energetically unfavorable ($E_b=25.6$ eV/cell). Hence, the metallic $(C_{60}O)_{\text{pol}}@(14,0)$ or smaller $(C_{60}O)_{\text{pol}}@(n,0)$ ($n < 14$) may be difficult to synthesize from a point of view of thermodynamics. But the synthesis of a compound is not just determined by its thermodynamic stability.

As for $(C_{60}O)_{\text{pol}}@(16,0)$, the nearest distance between the two constituents is about 2.9 Å, larger than that of $(C_{60}O)_{\text{pol}}@(14,0)$. The interaction between the two constituents has become weaker relative to that of $(C_{60}O)_{\text{pol}}@(14,0)$, so the basic band characteristics are retained much for both SWCNT(16,0)-derived and the 1D $C_{60}O$ polymer-derived bands. Nevertheless, from Fig. 2 it can be seen that the two frontier bands of the 1D $C_{60}O$ polymer in $(C_{60}O)_{\text{pol}}@(16,0)$ are elevated obviously compared with those in the isolated 1D $C_{60}O$ polymer. Moreover, the HOB of $(C_{60}O)_{\text{pol}}@(16,0)$ is derived from that of the 1D $C_{60}O$ polymer, not from that of tube (16,0). These indicate that the interaction between two constituents has important influence on the structures and character of the frontier bands for the peapods with smaller tube diameters.

The calculated densities of states (DOS) for the isolated 1D $C_{60}O$ polymer and peapods are shown in Fig. 3. The projected DOS of the 1D $C_{60}O$ polymer is denoted by the shadow area. For the metallic peapod $(C_{60}O)_{\text{pol}}@(14,0)$, it can be seen that the DOS has sharp peak near the Fermi level and is about 210 states $eV^{-1} \text{ cell}^{-1}$, which is almost contributed from the two nearly degenerated flat bands derived mainly from the 1D $C_{60}O$ polymer. Although large DOS may be favorable to the high temperature superconductivity, the narrow bands can lead to strong electron–electron interaction and suppress the superconducting phase-transition. The DOS at the Fermi level are completely contributed from the corresponding carbon nanotubes for $(C_{60}O)_{\text{pol}}@(10,10)$ and $(C_{60}O)_{\text{pol}}@(12,12)$. The wider frontier bands lead to smaller DOS, less than 8 states $eV^{-1} \text{ cell}^{-1}$. These values are smaller than those of the alkali metal doped C_{60} crystals

Table 2
Calculated electronic properties of the peapods (in eV). HOCO is the highest occupied crystal orbital and LUCO is the lowest unoccupied crystal orbital.

Peapods	HOCO	LUCO	E_g	HOB width	LUB width
$(C_{60}O)_{\text{pol}}@(14,0)$	−4.207	−4.207	0	–	–
$(C_{60}O)_{\text{pol}}@(16,0)$	−4.686	−4.174	0.512	0.128	0.639
$(C_{60}O)_{\text{pol}}@(18,0)$	−4.438	−4.389	0.049	0.971	0.952
$(C_{60}O)_{\text{pol}}@(20,0)$	−4.640	−4.210	0.430	0.735	0.710
$(C_{60}O)_{\text{pol}}@(22,0)$	−4.675	−4.237	0.438	0.857	0.849
$(C_{60}O)_{\text{pol}}@(10,10)$	−4.385	−4.385	0	–	–
$(C_{60}O)_{\text{pol}}@(12,12)$	−4.415	−4.415	0	–	–

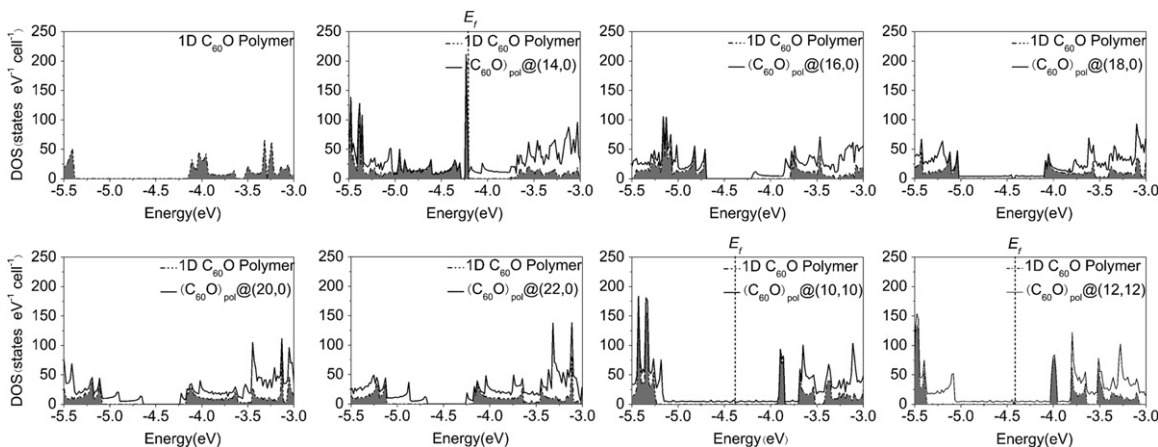


Fig. 3. Density of states for the 1D $C_{60}O$ polymer and the peapods.

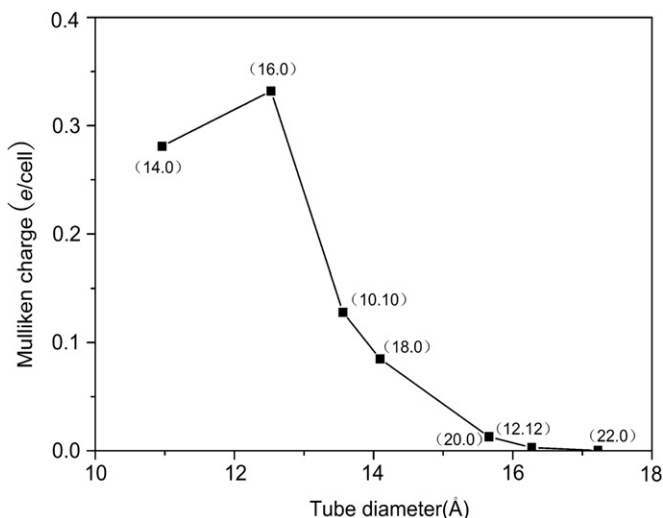


Fig. 4. Charge transfer from the SWCNTs to the 1D $C_{60}O$ polymer in the peapods.

(about 13–15 states/eV per C_{60}) [39,40]. Because of the smaller DOS, $(C_{60}O)_{\text{poi}}@(10,10)$ and $(C_{60}O)_{\text{poi}}@(12,12)$ thus may not be the candidates of superconducting material with phase transition temperature higher than those of alkali metal doped C_{60} crystals.

As for the semiconducting peapods, the DOS is also quite large (about 50 states $eV^{-1} \text{ cell}^{-1}$) near the top of valence band for the $(C_{60}O)_{\text{poi}}@(16,0)$ due to the 1D $C_{60}O$ polymer-derived flat HOB. The DOS near the top of valence band and bottom of conduction band for $(C_{60}O)_{\text{poi}}@(18,0)$, $(C_{60}O)_{\text{poi}}@(20,0)$ and $(C_{60}O)_{\text{poi}}@(22,0)$ are all less than 20 states $eV^{-1} \text{ cell}^{-1}$.

It can be seen that DOS distributions of the metallic zigzag peapods $(C_{60}O)_{\text{poi}}@(14,0)$, the semiconductive zigzag $(C_{60}O)_{\text{poi}}@(n,0)$ ($n > 14$) and the metallic armchair $(C_{60}O)_{\text{poi}}@(m,m)$ ($m = 10, 12$) are quite different from each other due to different band structures. Moreover, the shadow area shifts from the highest occupied bands and toward the lowest empty bands with increasing of the SWCNT diameters for the peapods. This is because the 1D $C_{60}O$ polymer-derived bands go down with increasing of the SWCNT diameters as already mentioned.

We also roughly describe the charge population of these peapods with Mulliken charge population method supplied by CRYSTAL06 program. It is found that there exists electron transfer from the tube to the inner 1D $C_{60}O$ polymer for the peapods studied as shown in Fig. 4. The charge transfer direction in these peapods is consistent with those in the C_{60} peapods [41], the C_{36}

peapods [42] and the carbon nanowires [25,26]. The peapods with smaller tube diameters form the polarity systems. The outside wall of the SWCNTs may be favorable to attack by the nucleophilic species.

3.4. Mobility

In order to understand more about the transport properties of these peapods qualitatively, the mobility of charge carriers is calculated based on the deformation potential (DP) approach [43], which has been successfully applied to 1D conducting polymer [44], DNA stack [45], graphene nanoribbons [46] and so on. With the DP and effective mass approximation, the mobility of the 1D systems can be expressed as follows [45,47]:

$$\mu = \frac{eh^2C}{(2\pi k_B T)^{1/2} |m^*|^{3/2} E_1^2} \quad (3)$$

where C is the stretching modulus of 1D crystal, m^* are the effective mass of electron or hole, T is the temperature and E_{1c} and E_{1v} are the DP constants of conduction band and valence band for the semiconducting peapods, respectively. As for the metallic peapods, E_1 is the DP constant at Fermi level. The effective mass can be obtained from $m^* = \hbar^2 [\partial^2 E / \partial k^2]^{-1}$. C is obtained from $C = a_0 \partial^2 E / \partial a^2 |_{a=a_0}$, where a_0 is the cell constant of 1D crystal. DP constant E_1 can be obtained from the equation $\delta\epsilon = E_1 \delta a / a_0 = E_1 \Delta$, then $E_1 = \delta\epsilon / \Delta$. In order to calculate C and E_1 , we also calculate the band structures and the energies of unit cell at six deformed lattice constants: $0.996a_0$, $0.998a_0$, $0.999a_0$, $1.001a_0$, $1.002a_0$ and $1.004a_0$. We fit the curve of strain energy with respect to the deformed lattice constants to obtain the stretching modulus C . From the changes of energy $\delta\epsilon$ with Δ , we get the values of DP constant of the peapods. Finally, substituting the values of the effective mass of electron and hole (m_e^* and m_h^*), E_1 and C into (3), we can get the mobilities of electrons and holes (μ_e and μ_h) at room temperature. The calculated results are listed in Table 3.

Based on the calculated results, the mobilities of holes and electrons for the four semiconductive peapods are in the range of 6.91×10^2 – $5.69 \times 10^4 \text{ cm}^2 \text{ V}^{-1} \text{ s}^{-1}$ and 5.63×10^3 – $1.11 \times 10^5 \text{ cm}^2 \text{ V}^{-1} \text{ s}^{-1}$, respectively. The mobility of electron is larger than that of hole by 1–2 order of magnitude except for $(C_{60}O)_{\text{poi}}@(20,0)$, indicating that the electrons are more favorable to movement in most of these semiconductive peapods. The 1D $C_{60}O$ polymer and $(C_{60}O)_{\text{poi}}@(16,0)$ have almost the same magnitude of hole mobility due to the 1D $C_{60}O$ polymer-derived HOBs in $(C_{60}O)_{\text{poi}}@(16,0)$. A theoretical study reports that the mobilities of some semiconductive SWCNTs can be improved after the

Table 3

Calculated mobilities of the peapods. μ_{e1} , μ_{e2} are the electron mobilities for bands 1 and 2 in the two conducting armchair peapods.

Peapods	μ_e ($\text{cm}^2 \text{V}^{-1} \text{s}^{-1}$)	μ_h ($\text{cm}^2 \text{V}^{-1} \text{s}^{-1}$)
(C ₆₀ O) _{poi} @(16,0)	9.614×10^4	6.909×10^2
(C ₆₀ O) _{poi} @(18,0)	1.104×10^5	5.182×10^3
(C ₆₀ O) _{poi} @(20,0)	5.629×10^3	5.693×10^4
(C ₆₀ O) _{poi} @(22,0)	1.113×10^5	7.856×10^3
	μ_{e1} ($\text{cm}^2 \text{V}^{-1} \text{s}^{-1}$)	μ_{e2} ($\text{cm}^2 \text{V}^{-1} \text{s}^{-1}$)
(C ₆₀ O) _{poi} @(10,10)	3.103×10^3	5.099×10^2
(C ₆₀ O) _{poi} @(12,12)	1.112×10^3	2.043×10^3

encapsulation of C₆₀ molecules [48]. With the same method the mobilities of charge carriers for the corresponding SWCNTs are also calculated for the comparison. The mobilities of charge carriers for the SWCNTs are some smaller than those for the corresponding peapods except for μ_h of (C₆₀O)_{poi}@(16,0), but the order of magnitude is also in the range of 10^2 – $10^5 \text{ cm}^2 \text{V}^{-1} \text{s}^{-1}$. This can be attributed to that the frontier bands of the peapods are all derived from SWCNTs except the HOB of (C₆₀O)_{poi}@(16,0).

For the metallic peapods, the electron mobility in the two partially filled bands is in the range of 5.10×10^2 – $3.10 \times 10^3 \text{ cm}^2 \text{V}^{-1} \text{s}^{-1}$ and smaller than that in the bottom of conducting bands for the semiconductive peapods.

The mobilities of charge carriers for the peapods are all in the range of 10^2 – $10^5 \text{ cm}^2 \text{V}^{-1} \text{s}^{-1}$ and not less than those for the corresponding SWCNTs, the combined systems may also be the candidates for high-mobility electronic materials.

4. Conclusion

In summary, we investigated the structures, energies and electronic properties as well as transport and elastic properties for the novel peapods—one dimensional C₆₀O polymer encapsulated in single-walled carbon nanotubes with various diameters using the SCF-CO method based on DFT in this paper. The distance between the two constituents has important influence on the structure shape and thermodynamic stability of these peapods. Among the peapods studied, the most stable ones are (C₆₀O)_{poi}@(18,0) and (C₆₀O)_{poi}@(10,10), for which the distance between the two constituent parts is in the Van der Waals scope between carbon atoms, 3.51 Å and 3.35 Å.

The interaction between the tubes and the 1D C₆₀O polymer also has strong influence on the electronic properties of the peapods with smaller diameter of the SWCNTs. The smallest peapod (C₆₀O)_{poi}@(14,0) studied becomes a metal with a zero energy gap. The zigzag peapods with larger tube diameters are all semiconductors, which are the same as the two constituents constructing the peapods.

The elastic moduli along the tube axis for the peapods are expected to be a little larger than those for the corresponding pristine SWCNTs and much larger than that for the isolated 1D C₆₀O polymer. This demonstrates that the encapsulation can make these combined systems stiffer than the two components. The mobilities of the peapods studied are all in the range of about 10^2 – $10^5 \text{ cm}^2 \text{V}^{-1} \text{s}^{-1}$. These peapods may be potential candidates for high-mobility electronic materials with stronger resistance to

the stress along the axis of the peapods due to the larger mobilities and moduli.

Acknowledgment

This work is supported by the Natural National Science Foundation of China (Grant no. 20873009).

References

- [1] S. Iijima, Nature 354 (1991) 56–58.
- [2] A.C. Dillon, K.M. Jones, T.A. Bekkedahl, C.H. Kiang, D.S. Bethune, M.J. Heben, Nature 386 (1997) 377–379.
- [3] S.S. Wong, E. Joselevich, A.T. Woolley, C.L. Cheung, C.M. Lieber, Nature 394 (1998) 52–55.
- [4] Z. Yao, H.W.C. Postma, L. Balents, C. Dekker, Nature 402 (1999) 273–276.
- [5] C. Zhou, J. Kong, E. Yenilmez, H. Dai, Science 290 (2000) 1552–1555.
- [6] A. Bachtold, P. Hadley, T. Nakanishi, C. Dekker, Science 294 (2001) 1317–1320.
- [7] G.U. Sumanasekera, B.K. Pradhan, H.E. Romero, K.W. Adu, P.C. Eklund, Phys. Rev. Lett. 89 (2002) 166801 (1–4).
- [8] A. Star, T. Han, J.P. Gabriel, K. Bradley, G. Gruner, Nano Lett. 3 (2003) 1421–1423.
- [9] R. Kitaura, N. Imazu, K. Kobayashi, H. Shinohara, Nano Lett. 8 (2008) 693–699.
- [10] K. Hirahara, S. Bandow, K. Suenaga, H. Kato, T. Okazaki, H. Shinohara, S. Iijima, Phys. Rev. B 64 (2001) 115420 (1–5).
- [11] J. Lu, S. Nagase, D. Yu, H. Ye, R. Han, Z. Gao, S. Zhang, L. Peng, Phys. Rev. Lett. 93 (2004) 116804 (1–4).
- [12] J. Kim, S. Park, J. Solid State Chem. 184 (2011) 2184–2189.
- [13] R. Carter, J. Sloan, A.I. Kirkland, R.R. Meyer, P.J.D. Lindan, G. Lin, M.L.H. Green, A. Vlandas, J.L. Hutchison, J. Harding, Phys. Rev. Lett. 96 (2006) 215501 (1–4).
- [14] R.R. Meyer, J. Sloan, R.E. Dunin-Borkowski, A.I. Kirkland, M.C. Novotny, S.R. Bailey, J.L. Hutchison, M.L.H. Green, Science 289 (2000) 1324–1326.
- [15] L. Guan, K. Suenaga, Z. Shi, Z. Gu, S. Iijima, Nano Lett. 7 (2007) 1532–1535.
- [16] B.W. Smith, M. Monthieux, D.E. Luzzi, Nature 396 (1998) 323–324.
- [17] X. Liu, T. Pichler, M. Knupfer, M.S. Golden, J. Fink, H. Kataura, Y. Achiba, K. Hirahara, S. Iijima, Phys. Rev. B 65 (2002) 045419 (1–6).
- [18] J. Fan, M. Yudasaka, R. Yuge, D.N. Futaba, K. Hata, S. Iijima, Carbon 45 (2007) 722–726.
- [19] D.A. Britz, A.N. Khlobystov, J. Wang, A.S. O’Neil, M. Poliakoff, A. Ardavan, G.A.D. Briggs, Chem. Commun. 40 (2004) 176–177.
- [20] P. Liu, Y.W. Zhang, H.J. Gao, C. Lu, Carbon 46 (2008) 649–655.
- [21] T. Miyake, S. Saito, Solid State Commun. 125 (2003) 201–204.
- [22] E. Hernández, V. Meunier, B.W. Smith, R. Rurali, H. Terrones, M.B. Nardelli, M. Terrones, D.E. Luzzi, J.-C. Charlier, Nano Lett. 3 (2003) 1037–1042.
- [23] D.A. Britz, A.N. Khlobystov, K. Porfyraakis, A. Ardavan, G.A.D. Briggs, Chem. Commun. 41 (2005) 37–39.
- [24] H. Bai, R. Du, W. Qiao, Y. Huang, J. Mol. Struct.-Theochem. 961 (2010) 42–47.
- [25] Y. Wang, Y. Huang, B. Yang, R. Liu, Carbon 44 (2006) 456–462.
- [26] Y. Wang, Y. Huang, B. Yang, R. Liu, Carbon 46 (2008) 276–284.
- [27] J. Chen, J. Dong, J. Phys.: Condens. Matter 16 (2004) 1401–1408.
- [28] M. Otani, S. Okada, A. Oshiyama, Phys. Rev. B 68 (2003) 125424 (1–8).
- [29] S. Okada, Phys. Rev. B 77 (2008) 235419 (1–7).
- [30] J.P. Perdew, K. Burke, M. Ernzerhof, Phys. Rev. Lett. 77 (1996) 3865–3868.
- [31] R. Dovesi, V.R. Saunders, C. Roetti, R. Orlando, C.M. Zicovich-Wilson, F. Pascale, B. Civalieri, K. Doll, N.M. Harrison, I.J. Bush, Ph. D’Arco, M. Llunell, CRYSTAL06 User’s Manual, University of Torino, Torino, 2006.
- [32] S. Okada, S. Saito, A. Oshiyama, Phys. Rev. Lett. 86 (2001) 3835–3838.
- [33] S. Okada, M. Otani, A. Oshiyama, Phys. Rev. B 67 (2003) 205411 (1–5).
- [34] A. Krishnan, E. Dujardin, T.W. Ebbesen, P.N. Yianilos, M.M.J. Treacy, Phys. Rev. B 58 (1998) 14013–14019.
- [35] J. Lu, Phys. Rev. Lett. 79 (1997) 1297–1300.
- [36] V.N. Popov, V.E. Van Doren, M. Balkanski, Phys. Rev. B 61 (2000) 3078–3084.
- [37] A.A. Farajian, M. Mikami, J. Phys.: Condens. Matter 13 (2001) 8049–8059.
- [38] J. Lu, S. Nagase, S. Zhang, L. Peng, Phys. Rev. B 68 (2003) 121402 (1–4).
- [39] S.C. Erwin, W.E. Pickett, Phys. Rev. B 46 (1992) 14257–14260.
- [40] K. Tanaka, Y. Huang, T. Yamabe, Phys. Rev. B 51 (1995) 12715–12720.
- [41] A. Rochefort, Phys. Rev. B 67 (2003) 115401 (1–7).
- [42] B. Yang, Y. Wang, Y. Huang, Chin. Sci. Bull. 51 (2006) 25–30.
- [43] J. Bardeen, W. Shockley, Phys. Rev. 80 (1950) 72–80.
- [44] G. Wang, Y. Huang, J. Phys. Chem. Solids 69 (2008) 2531–2534.
- [45] F.B. Beleznyay, F. Bogár, J. Ladik, J. Chem. Phys. 119 (2003) 5690–5695.
- [46] M. Long, L. Tang, D. Wang, L. Wang, Z. Shuai, J. Am. Chem. Soc. 131 (2009) 17728–17729.
- [47] Y. Huang, R. Liu, Chem. Res. Chin. U 7 (1991) 107–113.
- [48] R. Pati, L. Senapati, P.M. Ajayan, S.K. Nayak, J. Appl. Phys. 95 (2004) 694–697.